the curve labeled C in Fig. 5. The agreement with BST is good for $\Lambda < 3.5$. Equation (C7) gives good agreement with BST over about the same range of Λ as does the density expansion including terms through S_3.

The convergence of Eq. (C5)–(C7) will be used as a criteria to determine when the two-component quantum-mechanical generalization of these equations has broken down due to the plasma interaction.

---

[*] Work performed under the auspices of the U. S. Atomic Energy Commission.

[†] Work based in part on a Ph.D. dissertation submitted to the Department of Applied Science, University of California at Davis, 1972, which is available as University of California Lawrence Livermore Laboratory Report No. UCRL-51158.

[1] S. G. Brush, *Progress in High-Temperature Physics and Chemistry*, edited by C. A. Rouse (Pergamon, New York, 1967), Vol. 1, p 1; B. H. Armstrong, R. R. Johnston, P. S. Kelly, H. E. DeWitt, and S. G. Brush, *ibid.*, p. 231.

[2] M. McChesney, Can. J. Phys. **42**, 2473 (1964).

[3] G. M. Harris, Phys. Rev. **133**, A427 (1964).

[4] T. L. Hill, *Statistical Mechanics* (McGraw-Hill, New York, 1956), Chap. 5.

[5] J. E. Mayer, J. Chem. Phys. **18**, 1426 (1950).

[6] E. Meeron, J. Chem. Phys. 26, 804 (1957); J. Chem. Phys. **28**, 630 (1958).

[7] H. L. Friedman, Mol. Phys. 2, 23 (1959); J. Chem Phys. **32**, 1134 (1960); J. Chem. Phys. **32**, 1351 (1960).

[8] R. Abe, Prog. Theor. Phys. **22**, 213 (1959).

[9] S. G. Brush, H. E. DeWitt, and J. G. Trulio, Nucl. Fusion **3**, 5 (1963).

[10] E. W. Montroll and J. C. Ward, Phys. Fluids **1**, 55 (1958).

[11] H. E. DeWitt, J. Nucl. Energy C **2**, 27 (1961); J. Math. Phys. **3**, 1216 (1962); J. Math. Phys. **7**, 161 (1966); see also W. Ebeling, Physica (Utr.) **38**, 378 (1968); Physica (Utr.) **40**, 290 (1968); Physica (Utr.) **43**, 293 (1969); W. D. Kraeft and D. Kremp, Z. Phys. **208**, 475 (1968); H. J. Hoffman and W. Ebeling, W. Beitr. Plasmaphysik 8, 43 (1968); V. P. Kopyshev, Zh. Eksp. Teor. Fiz. 55, 1304 (1968) [Sov. Phys.-JETP 28, 684 (1969)].

[12] F. J. Rogers, H. C. Graboske, Jr., and H. E. DeWitt, Phys. Lett. A 34, 127 (1971); A. G. Petschek, Phys. Lett. A 34, 411 (1971).

[13] J. E. Mayer and M. G. Mayer, *Statistical Mechanics* (Wiley, New York, 1940).

[14] J. E. Mayer, *Equilibrium Statistical Mechanics* (Pergamon, New York, 1968), p. 88.

[15] H. E. DeWitt and H. C. Graboske, Jr. (unpublished).

[16] T. Nakayama and H. E. DeWitt, J. Quant. Spectrosc. Radiat. Transfer **4**, 623 (1964).

[17] A. Glasgold, W. Heckrotte, and K. Watson, Phys. Rev. **115**, 1374 (1959).

[18] F. J. Rogers, Phys. Rev. A 4, 1145 (1971).

[19] H. E. DeWitt, *Low Luminosity Stars*, edited by S. Kamar (Gordon and Breach, New York, 1969).

[20] F. J. Rogers, H. C. Graboske, Jr., and D. J. Harwood, Phys. Rev. A **1**, 1577 (1970).

[21] S. Larsen, J. Kilpatrick, E. Lieh, and H. Jordan, Phys. Rev. **140**, A129 (1965); M. E. Boyd, S. Y. Larsen, and J. E. Kilpatrick, J. Chem. Phys. **50**, 4034 (1969).

[22] J. O. Hershfelder, C. F. Curtiss, and R. B. Bird, *Molecular Theory of Gases and Liquids* (Wiley, New York, 1954).

[23] S. G. Brush, H. L. Sahlin, and E. Teller, J. Chem. Phys. **45**, 2102 (1966).

[24] J. G. Trulio and S. G. Brush, Phys. Rev. **121**, 1940 (1961).

[25] F. del Rio and H. E. DeWitt (unpublished).

PHYSICAL REVIEW A VOLUME 8, NUMBER 2 AUGUST 1973

Afterglow Studies in Helium-Cesium Mixtures*

R. S. Bergman[†] and L. M. Chanin

Department of Electrical Engineering, University of Minnesota, Minneapolis, Minnesota 55455

(Received 11 January 1973)

The time dependencies of the He^+, He_2^+, and Cs^+ ion densities have been measured during the decay period of a plasma produced in helium containing from $(10^{-6}–10^{-2})$% cesium. Analyses of the ion decay rates as a function of helium pressure indicate that Cs^+ is produced in the afterglow by collisions between neutral ground-state cesium atoms and He^+, He_2^+, and He(2 ^3S). The values of the rate constants measured at a gas temperature of $T_g = 415$ °K for these reactions are $k_2(He^+) = 3\times10^{-10}$ cm^3/sec, $k_3(He2\ ^3S) = 1\times10^{-9}$ cm^3/sec, and $k_4(He_2^+) = 2\times10^{-9}$ cm^3/sec. The reduced mobility of Cs^+ in helium at 415 °K was measured to be (15.5 ± 1) cm^2/V sec.

I. INTRODUCTION

Mass-spectrometer ion-sampling measurements were recently made on dc- and rf-excited cesium discharges.[1,2] Comparisons of the ion current signals of Cs^+, Cs_2^+, and Cs_3^+ with predictions based on a simplified reaction-kinetics scheme enabled estimates to be made of some of the rate constants for various ion production and loss processes. The interpretation of ion-sampling measurements obtained from active plasmas is quite complicated. Reasons for this involve considerations of ion transmission through plasma boundary sheaths and also, when present, the effects of phenomena such as striations in the discharge, etc. Furthermore, two assumptions used to solve the continuity equations involved may be questioned when considering processes in active plasmas. These assumptions are (a) that the charged particles have a Maxwellian velocity distribution and (b) that the higher-order diffusion modes of the spatial particle distribution can be neglected in comparison to the fundamental mode, which is a zeroth-order Bessel function for a cylindrical discharge tube.

The interpretation of ion-sampling results from decaying plasmas is, by comparison, much less complicated. The assumptions of a Maxwellian velocity distribution and a fundamental diffusion-mode spatial distribution are more easily satisfied in the late afterglow period. In addition, the electron energy decays to thermal energies so that the charged-particle production processes involving electron impact can be neglected. In the late stages of the plasma decay period, diffusion and linear volume losses will dominate volume-recombination losses.

To our knowledge no measurements on decaying plasmas produced in cesium or cesium–noble-gas mixtures have been reported. The reasons for this are probably related to the comparative difficulties encountered in performing measurements on a highly reactive gas. The main purpose of this investigation was to measure the processes by which Cs^+ is produced in the afterglow and also to measure the mobility of Cs^+ in helium. The reaction-rate constants for these processes were measured. Satisfactory system performance was first evaluated in pure helium before cesium was introduced. Since the $D_a p_0$ values for He^+ and He_2^+ in helium (D_a -ambipolar diffusion coefficient) are well established and the three-body conversion frequency for $He^+ + 2He \rightarrow He_2^+ + He$ is also well known, proper equipment performance is readily determined.[3,4]

II. EXPERIMENTAL METHOD

The time dependencies of the ions during the afterglow are measured using an electric quadrupole mass spectrometer which samples ions diffusing to the walls of the discharge tube.[5] The experimental tube is mounted on a gas-handling system similar to that previously described.[6] A block diagram of the vacuum system is shown in Fig. 1. That part of the system enclosed by the dashed lines is baked at 620 °K for about 36 h prior to the measurements. The pressure controller automatically compensates for gas loss through the sampling orifice by operating a servo-controlled leak valve which is connected to the gas supply. In this way a constant preset pressure is maintained in the system. The cataphoresis tube is used to purify the research-grade helium gas used in the studies.[7,8] This procedure was necessary before self-consistent data could be obtained in pure helium.

The cesium had a reported purity of 99.8%. The cesium still is a modification of one similar to that described by Fendley.[9] A temperature-controlled oil bath is used to determine the cesium-source pressure. For the afterglow studies the discharge-tube temperature was maintained at least 50 °C above the source temperature. The cesium density in the discharge tube is determined using extensive thermocouple measurements and vapor-pressure data.[10]

Figure 2 shows a schematic of the discharge

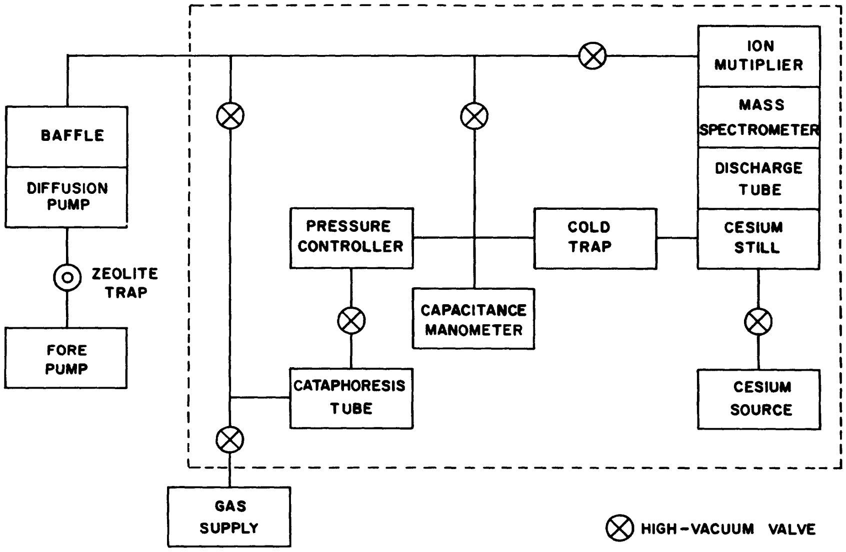

FIG. 1. Block diagram of the gas-handling station.

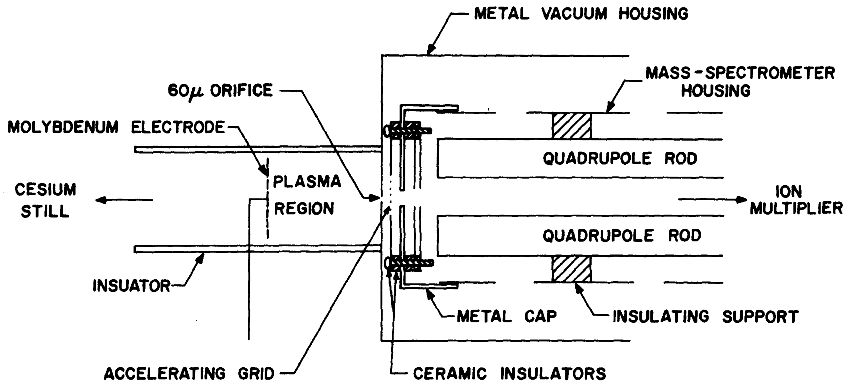

FIG. 2. Schematic drawing of the plasma cell and quadrupole mass-spectrometer region.

tube and quadrupole mass-spectrometer regions. The discharge region is a glass cylinder with metal endplates. The 60-μ-diam sampling orifice is drilled in the center of a 30-μ-thick stainless-steel sheet. A perforated molybdenum electrode placed about 3 cm from the orifice plate defines the plasma region. To reduce desorption by the discharge of impurities from the discharge cell walls a layer of molybdenum is sputtered on the walls. A series of successive sputterings of both end plates is necessary before self-consistent data can be obtained. This is presumably required to provide clean conditions in the orifice region. In this manner, a helium afterglow with less than 0.5% total impurity-ion signals is obtained.

The discharge is produced by a high-voltage dc pulse applied between the discharge-tube electrodes. The discharge pulse could be varied from 10 μsec to 10 msec, while the period of the discharge could be varied from 100 μsec to 10 sec. The usual mode of operation involved a 1.0-msec pulse with a 32-msec period. Ions emerging from the quadrupole are detected by a 14-stage RCA C7187K ion multiplier.

Figure 3 shows a schematic of the measuring system. The anode pulses are amplified by the wide-band amplifier and then fed into a discriminator having a threshold voltage variable from − 50 to − 550 mV. The threshold voltage is chosen such that the signal-to-noise ratio is maximized. Logic pulses from the discriminator pass into the multichannel scalar. The scalar contains a 400-channel memory with a capacity of 10^6 counts per channel. The time-base generator is used to advance the channels of the scalar from channel to channel. The number in each channel corresponds to the ion signal intensity during that time interval in the afterglow. This type of electronic detection is the same as that described by Veatch and Oskam.[11]

III. AFTERGLOW PROCESSES AND RELEVANT THEORY

In this section the equations which describe the time dependencies of the helium ions, helium metastable particles, and cesium ions during the decay period of the plasma are considered. The derivation of the equations for helium plasmas has been discussed previously.[4,11] In the present study of He-Cs mixtures the following conditions are as-

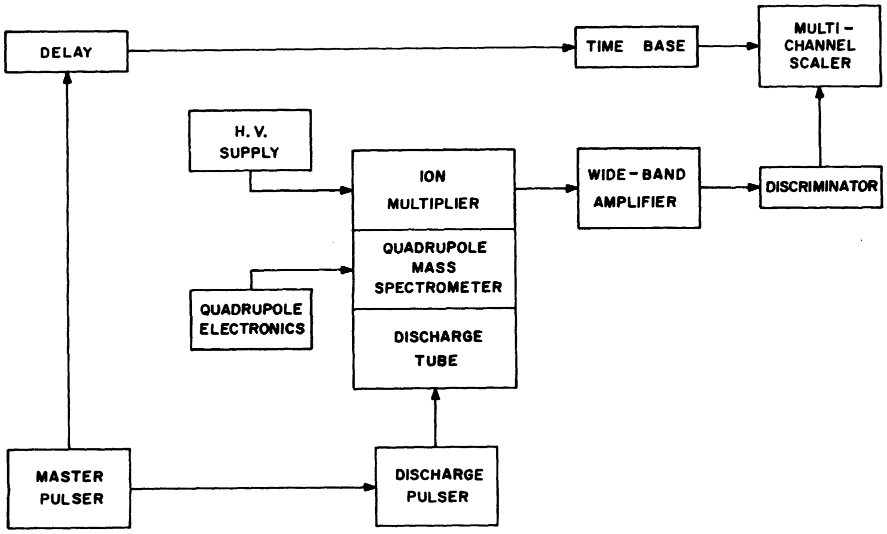

FIG. 3. Electronic measuring system schematic.

sumed.

(i) He^+ ions are lost by ambipolar diffusion, by conversion into He_2^+ by the reaction

$$He^+ + 2He \rightarrow He_2^+ + He, \tag{1}$$

and by the charge exchange process

$$He^+ + Cs \rightarrow Cs^+ + He^m. \tag{2}$$

(ii) The metastable helium particles He^m are lost by diffusion and conversion into Cs^+ by the Penning process

$$He^m + Cs \rightarrow Cs^+ + He + e \quad . \tag{3}$$

He^m is produced in the afterglow by process (2).

(iii) He_2^+ ions are lost by ambipolar diffusion and the charge exchange reaction

$$He_2^+ + Cs \rightarrow Cs^+ + 2He \quad . \tag{4}$$

The molecular helium ion is produced by process (1).

(iv) Cs^+ ions are lost by diffusion to the walls of the container and produced by processes (2)–(4).

(v) Recombination losses of He^+, He_2^+, and Cs^+ with electrons are negligible in comparison with the other loss processes, especially in the late afterglow.

(vi) The production of He^+ by the process

$$He^m + He^m \rightarrow He^+ + He + e \tag{5}$$

is neglected, since under most conditions of the present experiment this production process could not be detected owing to the destruction of the metastable atoms by the cesium atoms. At very low cesium concentrations, however, the production of He^+ by process (5) could be observed in the late afterglow. This process has been discussed by Veatch and Oskam.[11]

The continuity equations of helium metastable atoms, helium ions, and cesium ions, with the above conditions applied, are given by

$$\frac{\partial n_1(\vec{r}, t)}{\partial t} = D_{a1}\nabla^2 n_1(\vec{r}, t) - \nu_1 n_1(\vec{r}, t) - \nu_2 n_1(\vec{r}, t) \quad , \tag{6}$$

$$\frac{\partial M(\vec{r}, t)}{\partial t} = D_m \nabla^2 M(\vec{r}, t) - \nu_3 M(\vec{r}, t) + \nu_2 n_1(\vec{r}, t) \quad , \tag{7}$$

$$\frac{\partial n_2(\vec{r}, t)}{\partial t} = D_{a2}\nabla^2 n_2(\vec{r}, t) - \nu_4 n_2(\vec{r}, t) + \nu_1 n_1(\vec{r}, t) \quad , \tag{8}$$

$$\frac{\partial n_3(\vec{r}_1 t)}{\partial t} = D_{a3}\nabla^2 n_3(\vec{r}, t) + \nu_2 n_1(\vec{r}, t) + \nu_3 M(\vec{r}, t) + \nu_4 n_2(\vec{r}, t) \quad . \tag{9}$$

Here M, n_1, n_2, and n_3 are the densities of metastable helium particles, atomic-helium ions, molecular-helium ions, and atomic-cesium ions, respectively; D_m is the diffusion coefficient of M; D_{a1}, D_{a2}, and D_{a3} are the ambipolar diffusion coefficients of the atomic-helium ions, molecular-helium ions, and atomic-cesium ions, respectively; ν_i ($i = 1, 2, 3, 4$) is the conversion frequency related to process (1).

The solutions of the continuity equations are obtained by assuming that the particle densities are zero at the walls of the plasma cylinder. Only the fundamental diffusion-mode solutions are considered, since the effect of higher-order modes on the data can be assumed to be negligible in the late afterglow. Under these conditions the time-dependent solutions of Eqs. (6)–(9) are rather simple functions.

For particles which are not produced during the decay period, the time dependence of the fundamental mode is a single exponential function. The relevant time constant is directly related to the loss processes of the particle. If the particle is also produced during the decay period, its time dependence is given by the sum of exponential functions which have different time constants. One time constant is related to the loss process of the particle, while others describe the loss of the reactant which is involved in the production of the particle. The final decay of the particles will be determined by the largest time constant.

It can be readily shown that the time constant τ_i related to the loss processes of n_1, M, n_2, and n_3, for Eqs. (6)–(9) are given by

$$1/\tau_1 = D_{a1}/\Lambda^2 + \nu_1 + \nu_2 \quad , \tag{10}$$

$$1/\tau_m = D_m/\Lambda^2 + \nu_3 \quad , \tag{11}$$

$$1/\tau_2 = D_{a2}/\Lambda^2 + \nu_4 \quad , \tag{12}$$

$$1/\tau_3 = D_{a3}/\Lambda^2 \quad . \tag{13}$$

The characteristic diffusion length Λ of the cylindrical plasma container of radius R and length L is given by

$$1/\Lambda^2 = (2.4/R)^2 + (\pi/L)^2 \quad . \tag{14}$$

Equations (10)–(13) express, for a given value of Λ, the expected time dependence of He^+, He^m, He_2^+ and Cs^+ for helium-cesium mixtures. As will be explained more fully in Sec. V, He^m will refer specifically to $He(2\,^3S)$. The values used for the diffusion coefficient of He^m, D_m, and the various reaction rates involving He^m in helium are those reported by Phelps.[12] The values for $D_{a1}p_0$, $D_{a2}p_0$, and ν_1 are those reported by Gerber, Sauter, and Oskam.[3] Substituting these results in Eqs. (10)–(13), values for ν_2, ν_3, and ν_4 can be obtained by measuring the p_0/τ values of He$^+$, He$_2^+$ and Cs$^+$ as a function of p_0 at various cesium concentrations.

The collision frequency ν of a given process involving a neutral cesium atom equals the rate constant of that process k times the cesium density n_{Cs}, i.e., $\nu = kn_{Cs}$. Thus, the rate constants k_2, k_3, and k_4 of processes (2)-(4) can be easily obtained from the measured values of ν_2, ν_3, and ν_4.

The ambipolar diffusion coefficient D_{a3} of Cs$^+$ in helium can be measured by plotting p_0/τ_3 as a function of p_0. The value for the normalized mobility of Cs$^+$ in helium is then obtained from the relation

$$\mu_0 = \frac{7.63\, D_{a3} p_0}{T_g}\ \mathrm{cm^2/V\,sec}\ , \qquad (15)$$

where T_g is the Maxwellian temperature of the ions, which is assumed to be equal to the gas temperature.[13]

IV. RESULTS

Measurements in helium-cesium mixtures require the operation of the discharge cell at elevated temperatures. In the present measurements the cell temperature was typically 400-500 °K. If the charge exchange frequency ν_2 of He$^+$ into Cs$^+$ is to be measured accurately, it is necessary to determine whether the formation of He$_2^+$ from He$^+$ is strongly temperature dependent. For this reason, measurements were made on pure helium at elevated temperatures. On the basis of these results, which covered only the relatively small temperature range of interest (300-500 °K), we conclude that the conversion frequency of He$^+$ into He$_2^+$ is not strongly temperature dependent.[14] The results, moreover, indicate that over this temperature range the ion diffusion coefficients vary approximately linearly with temperature.

Figure 4 shows an example of time dependencies of He$^+$, He$_2^+$, and Cs$^+$ obtained at $p_0 = 3.0$ Torr and $p_{Cs} = 1\times10^{-5}$ Torr. The gas temperature T_g was 415 °K. The solid lines drawn through the data shown the average exponential time dependencies of the ions in the late afterglow. Usually the time constant could be determined to within ± 5%. No Cs$_2^+$ signal was detected. This fact is explained by the negligible contribution of the three-body conversion reaction $\mathrm{Cs^+ + He + Cs \rightarrow Cs_2^+ + He}$ at these small cesium pressures.[15]

A series of measurements of p_0/τ such as obtained from Fig. 4, at various helium pressures, for two values of cesium density, are plotted in Figs. 5 and 6. Figure 5 shows p_0/τ values for He$^+$, He$_2^+$, and Cs$^+$ as a function of helium pressure at a very low concentration of cesium ($p_{Cs} = 2\times10^{-8}$ Torr) at a cell temperature of 300 °K. At this cesium concentration the plot of p_0/τ_1 and p_0/τ_2 as a function of p_0 is essentially equal to that obtained in pure helium. Hence the losses of He$^+$ and He$_2^+$ due to processes (2) and (4) are negligible in comparison to the diffusion loss. Enough Cs$^+$ was detected in the decay period, however, to obtain a value of p_0/τ of Cs$^+$ at all helium pressures.

Figure 6 is similar to Fig. 5, except that the cesium pressure is almost three orders of magnitude larger ($p_{Cs} = 10^{-5}$ Torr) and the cell temperature is 415 °K. Here the charge exchange reaction, pro-

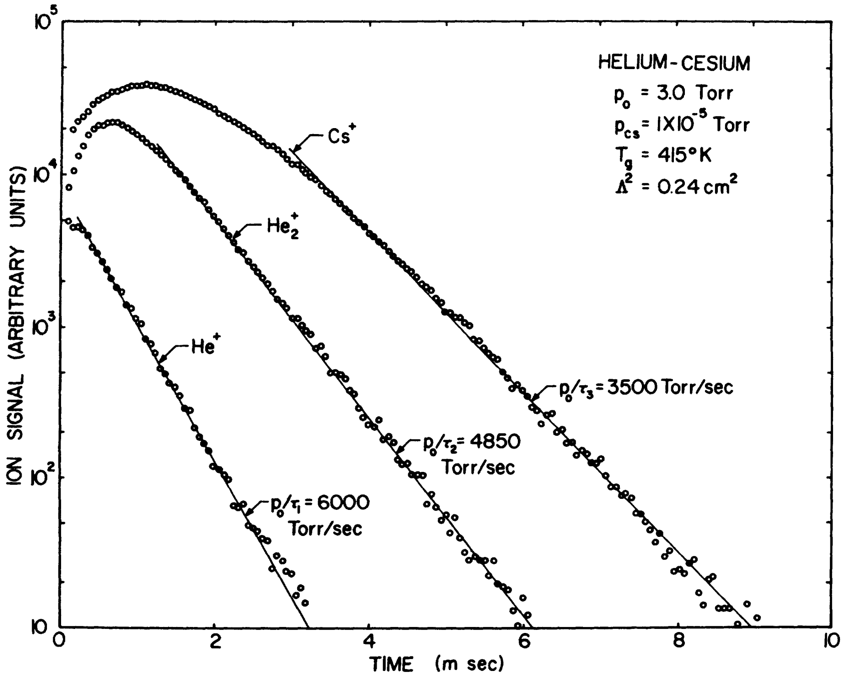

FIG. 4. Time dependence of the He$_2^+$ and Cs$^+$ density during the decay period of a plasma produced in helium-cesium mixtures at a normalized pressure of 3.0 Torr and a gas temperature of 415 °K. The cesium pressure was ~ 1×10^{-5} Torr.

cess (4), is readily apparent by the linear rise of p_0/τ_2 with p_0 above 3 Torr. The dependence of p_0/τ on p_0 for Cs^+ in Fig. 6 gives evidence of both the Penning-ionization reaction [process (3)] and the diffusion loss of Cs^+ in helium. A comparison of the measured values of p_0/τ for He^+, He_2^+, and Cs^+ in Figs. 5 and 6 with Eqs. (10)–(13) and other investigations (theoretical and experimental) will be discussed in the next section.

V. DISCUSSION OF RESULTS

Information concerning process (2) will be contained in the plot of p_0/τ_1 as a function of the normalized helium pressure p_0. From Eq. (10) and data from Ref. 3,

$$p_0/\tau_1 = 1800 + 80p_0^3 + \nu_2 p_0 \qquad (16)$$

for $\Lambda^2 = 0.24$ cm^2 and $T_g = 300$ °K. Since $\nu_2 = k_2 n_{Cs}$, p_0/τ_1 should exhibit a superimposed linear and cubic pressure dependence if n_{Cs} is constant.

The fact that the experimental values of p_0/τ_1 vs p_0 shown in Fig. 5 are essentially equal to the reported dependence for pure helium indicates that ν_2 is negligible at $p_{Cs} = 2\times10^{-8}$ Torr. The effect on p_0/τ_1 due to loss of He^+ by charge exchange with Cs (ν_2) shown in Fig. 6 is observable. However, it is difficult to obtain accurate estimates of ν_1, since the inherent cubic pressure dependence of p_0/τ_1 dominates the linear term above 2 Torr. Below 1 Torr, where the cubic pressure term is minimized, the measurements of p_0/τ_1 were not accurate. A plot (not shown) of p_0/τ_1 as a function of p_0 at $p_{Cs} = 10^{-4}$ Torr did substantiate the cited value of ν_2, since at this cesium pressure ν_2 is ten times larger than that shown in Fig. 6. From a series of p_0/τ_1 curves such as given in Figs. 5 and 6, at various cesium concentrations, a value of $k_2 \sim (3\pm1.5)\times10^{-10}$ cm^3/sec was obtained for the reaction-rate constant of process (2) at 415 °K.

Notice that the zero-pressure value extrapolated for p_0/τ_1 is larger in Fig. 6 than in Fig. 5. The diffusion coefficient D_{a1} of He^+ in helium is expected to increase with temperature. Since the temperature in Fig. 6 is 115 °C higher than that in Fig. 5, the increase of the zero-pressure value of p_0/τ_1 is explained. The actual temperature dependence of D_{a1} was not easily determined, however, since zero-pressure p_0/τ_1 values were extrapolated from measurements above 1 Torr.

Previous experiments of the charge exchange reaction between He^+ and Cs have involved beam studies.[16–18] These studies have investigated the cross section of the reaction for He^+ beam energies ranging from 10 eV to 25 keV. The results show that

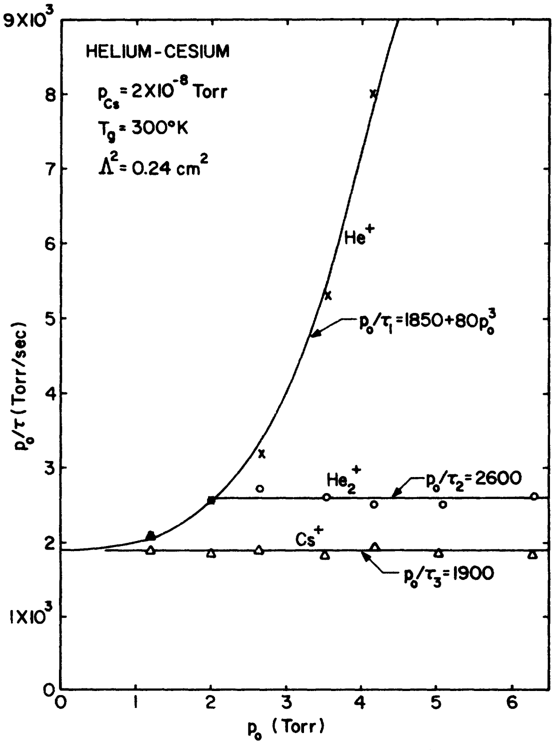

FIG. 5. Measured values of p_0/τ for He^+, He_2^+, and Cs^+ as a function of normalized helium pressure. The gas temperature was 300 °K and the cesium pressure 2×10^{-8} Torr.

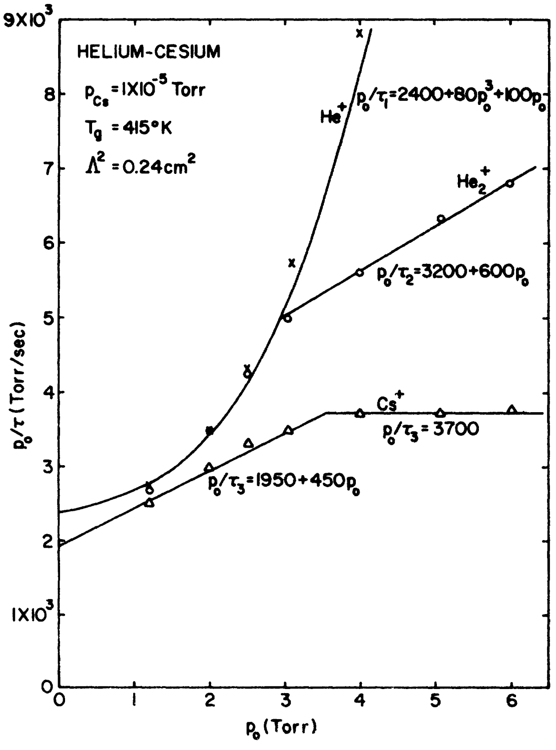

FIG. 6. Measured values of p_0/τ for He^+, He_2^+, and Cs^+ as a function of normalized helium pressure. The gas temperature was 415 °K and the cesium pressure 1×10^{-5} Torr.

the cross section increases with energy up to a beam energy of about 1.5 keV and then decreases. The charge exchange cross section measured by Peterson and Lorents[16] at 10 eV is $\sigma_1 = 0.67\times10^{-14}$ cm^2. In the afterglow $k_1 = \sigma_1 \bar{v}_{\text{therm}}$: hence the measured value of k_1 corresponds to $\sigma_1 = 0.16\times10^{-14}$ cm^2, which is a factor of about 4 below that reported at 10 eV. Since σ_1 decreases with decreasing energy, we conclude that the agreement with previous investigations is reasonable.

The charge exchange of He_2^+ with Cs [reaction (4)] can be measured by plotting p_0/τ_2 as a function of helium pressure above a certain critical pressure (for $\Lambda^2 = 0.24$ cm^2 this pressure is approximately 2.2 Torr). Using Eq. (14) and data from Ref. 3,

$$p_0/\tau_2 = 2700 + \nu_4 p_0 \qquad (17)$$

at 300 °K. Thus, for a given cesium concentration p_0/τ_2 should vary linearly with pressure above a certain critical pressure. The range of cesium concentration needed to estimate the reaction coefficient k_4 is limited. The concentration must be high enough to observe a significant rise in p_0/τ_2 with pressure, i.e., ν_4 must be of the order of $D_{a2}p_0$. On the other hand, the cesium density must be low enough to observe p_0/τ_2 separate from p_0/τ_1. The two slopes will be identical if $p_0/\tau_2 > p_0/\tau_1$, since He_2^+ is produced only from He^+.

The measured values of p_0/τ_2 in Fig. 5 are independent of pressure above 2.2 Torr. Thus, at this low cesium concentration, the charge exchange frequency between He_2^+ and Cs is negligible compared to the diffusion rate of He_2^+.

Figure 6 shows the linear p_0/τ_2 dependence on p_0 above the critical pressure when ν_4 is much larger than that in Fig. 5. The value of the slope of p_0/τ_2 in Fig. 6 (600 sec^{-1}) and the known cesium concentration leads to a measured value of $k_4 \simeq 2\times10^{-9}$ cm^3/sec at 415 °K. This value for k_4 was measured to within a factor of 2 for different cesium concentrations up to $p_{Cs} \simeq 10^{-4}$ Torr.

Extrapolation of the best fit to the measured value of p_0/τ_2 to zero pressure yields a value of 3200 Torr/sec, which is proportional to the value of D_{a2}. This value is higher than that measured in Fig. 5. As was the case for D_{a1}, this indicates that D_{a2} increases with increasing gas temperature.

No previous measurements have been made of the charge exchange constant k_4 for the reaction

$$He_2^+ + Cs \rightarrow Cs^+ + 2He \ . \qquad (4)$$

This general type of process, however, has been studied by other investigators.[19] Measurements of the rate coefficient for the above reaction provides a good comparative test of the theory of Gioumousis and Stevenson,[20] which assumes that the total cross section is determined by the ion-induced dipole interaction

$$V(r) = e^2\alpha/2r^4 \ , \qquad (18)$$

where e is the electronic charge and α is the polarizability of Cs. Gioumousis and Stevenson have shown that when a Maxwellian velocity distribution can be assumed,

$$k_4 = 2\pi(e^2\alpha/M_r)^{1/2} \ ,$$

where M_r is the reduced mass. Using published values for the polarizability[21] gives $k_4 \simeq 6\times10^{-9}$ cm^3/sec for the theoretical value of the rate constant of reaction (4). This value for k_4 is about a factor of 3 higher than the measured value.

Penning ionization of Cs by the metastable helium particles [especially He($2\,^3S$)], process (3), is expected to be a significant production mechanism. In the present experimental study the p_0/τ_m values could not be measured directly, since no detection methods for metastable particles were available. The Penning-ionization frequency ν_3 can be measured indirectly, however, under certain conditions.

From Fig. 4 and data from Ref. 12,

$$p_0/\tau_m = 1950 + \nu_3 p_0 \qquad (19)$$

at $T_g = 300$ °K. Equation (19) refers only to He($2\,^3S$), since the singlet, He($2\,^1S$), has an additional quadratic pressure dependence. As noted in Sec. III, the time constant of the observed particle will be determined by the decay of the producing particle when the producing particle time constant is larger than that of the observed particle. Thus, if $p_0/\tau_3 = D_{a3}p_0/\Lambda^2$ is larger than $D_m p_0/\Lambda^2$ (D_{a3} is expected to be comparable to that of D_{a2}), and if the concentration of cesium is sufficiently low, the decay of Cs^+ in the afterglow will be observed to follow that of He($2\,^3S$). This effect is similar to the decay of He_2^+ being determined by that of He^+ at low pressure.

Figure 5 shows that even at this low concentration of cesium in helium (~0.01 ppm) sufficient cesium ions were detected to obtain a value for p_0/τ. The Penning-ionization frequency of He($2\,^3S$) with Cs (ν_3) is too small to significantly change the p_0/τ_m value owing to diffusion [1950 Torr/sec in Eq. (19)]. Hence, the observed p_0/τ value of Cs^+ in Fig. 5 is equal to the value of p_0/τ_m [Eq. (19), with $\nu_3 \approx 0$].

From the p_0/τ measurement of Cs^+ as a function of p_0 shown in Fig. 6, values for both the rate constant of He($2\,^3S$) + Cs → Cs^+ + He + e and the mobility of Cs^+ in helium can be obtained. The slope (450 sec^{-1}) of p_0/τ_m vs p_0 is equal to the Penning-ionization frequency ν_3 of He($2\,^3S$) with Cs^+. From this value of ν_3 and others measured at different values of p_{Cs} up to 10^{-4} Torr, a value of $k_3 \simeq 1\times10^{-9}$ cm^3/

sec is obtained, which is accurate to within a factor of 2. The zero-pressure value of p_0/τ_m is equal to $D_m p_0/\Lambda^2$.

No measurements of the Penning-ionization rate of Cs$^+$ by helium metastables have been reported. Ionization cross sections for collisions of He($2\,^3S$) with Ar, Kr, Xe, H_2, O_2, N_2, and CO have been measured by Sholette and Muschlitz.[22] Bell, Dalgarno, and Kingston[23] have derived a theoretical estimate for this type of reaction. Assuming long-range interactions, they calculate values which are in reasonable agreement with those measured by Sholette and Muschlitz. For $\mathrm{He}(2\,^3S)+\mathrm{Cs}\rightarrow\mathrm{Cs}^+ +\mathrm{He}+e$ at 300 °K, Bell, Dalgarno, and Kingston calculate a value of $k_3 = 0.97\times10^{-9}$ cm^3/sec. This value is an excellent agreement with that obtained in the present study.

The mobility of Cs$^+$ in helium is evaluated by measuring the p_0/τ_3 value when $p_0/\tau_m > p_0/\tau_3$, i.e., high enough cesium concentration and helium pressure to ensure that the time constant for the decay of Cs is larger than that of He($2\,^3S$). The values of p_0/τ_3 are independent of p_0 above 4 Torr in Fig. 6. By Eq. (13), $D_{a3}p_0$ can be evaluated from p_0/τ_3. Using Eq. (15), the reduced mobility (760 Torr and 273 °K) is estimated to be $\mu_0 = 15.5 \pm 1$ cm^2/V sec at $T_g = 415$ °K.

The present mobility value provides a test of Langevin's theory of ion mobility.[24] Langevin's polarization limit of the mobility is given by

$$\mu_0 = \frac{0.5105}{[\rho(K-1)]^{1/2}}\left(1+\frac{M}{m_i}\right)^{1/2}, \qquad (20)$$

where ρ is the gas density, K is the dielectric constant (of He in this case[25]), and M and m_i are the mass of He and Cs$^+$, respectively. Equation (20) yields $\mu_0 \simeq 16$ cm^2/V sec for the mobility of Cs$^+$ in helium. This value is in good agreement with present experimental results.

The mobility of Cs$^+$ in helium was previously reported in Tyndall's classic investigations of ionic mobilities.[26] Tyndall reported a value of $\mu_0 \sim 18$ cm^2/V sec at temperatures comparable to that of the present study. In these studies, mass identification of ions was not possible, however.

TABLE I. Comparison of present measurements of the reaction-rate coefficients for the production Cs$^+$ in He-Cs afterglows and the mobility of Cs$^+$ in helium with previous studies and/or theory. The present values of the rate coefficients and the mobility of Cs$^+$ refer to a gas temperature of $Tg = 415$ °K.

Coefficient k (10^9 cm^3/sec)	This work	Previous studies	Theoretical calculations
k_2	0.3 ± 0.15	1.3(10 eV)[a]	...
k_3	$2.0^{+2.0}_{-1.0}$	...	6.0[b]
k_4	$1.0^{+1.0}_{-0.5}$	...	0.97[c]
μ_0 (cm^2/V sec)	15.5 ± 1	18.0[d]	16.0[e]

[a] Reference 16.
[b] Reference 20.
[c] Reference 23.
[d] Reference 26.
[e] Reference 24.

It is interesting to note that other investigators using similar experimental techniques to study helium-hydrogen-xenon mixtures have obtained a mobility value $\mu_0 \sim 16$ cm^2/V sec for XeH$^+$ in helium at room temperature.[27] The difference in mass between Cs$^+$ and XeH$^+$ is negligible. Mobility values for Hg$^+$ and U$^+$ in helium have recently been given by Johnson and Biondi.[28] These authors report that at 292 °K the mobility of Hg$^+$ is $\mu_0 \sim 19.4 \pm 0.5$ cm^2/V sec and that of U$^+$ is $\mu_0 \sim 16.0 \pm 0.5$ cm^2/V sec. Clearly these results imply that problems remain in understanding simple ionic mobilities.

In summary, the values for the rate coefficients and mobility measured in the present investigation are listed in Table I, with relevant values from other investigations and theoretical calculations.

ACKNOWLEDGMENTS

The authors are indebted to H. J. Oskam and other members of the plasma physics group for many helpful discussions during the course of this work.

---

*Sponsored in part by the Office of Naval Research, Power Branch.

†Present address: General Electric Company, Nela Park, Cleveland, Ohio 44112.

[1] R. S. Bergman and L. M. Chanin, Appl. Phys. Lett. **16**, 426 (1970).

[2] R. S. Bergman and L. M. Chanin, J. Appl. Phys. **42**, 4208 (1971).

[3] R. A. Gerber, G. F. Sauter, and H. J. Oskam, Physica (Utr.) **32**, 2173 (1966).

[4] A. V. Phelps and S. C. Brown, Phys. Rev. **86**, 102 (1952).

[5] G. F. Sauter, R. A. Gerber, and H. J. Oskam, Rev. Sci. Instrum. **35**, 412 (1964).

[6] D. Alpert, J. Appl. Phys. **24**, 860 (1953).

[7] R. Riesz and G. H. Dieke, J. Appl. Phys. **25**, 1961 (1954).

[8] J. P. Gaur and L. M. Chanin, J. Appl. Phys. **182**, 167 (1969).

[9] J. R. Fendley, Jr., Rev. Sci. Instrum. **35**, 905 (1964).

[10] J. B. Taylor and I. Langmuir, Phys. Rev. **51**, 753 (1937).

[11] G. E. Veatch and H. J. Oskam, Phys. Rev. **184**, 202 (1969).

[12] A. V. Phelps, Phys. Rev. **99**, 1307 (1955).

[13] Equation (19) is derived using the Einstein relation $D_+/\mu_+ = kT_+/q$ and the assumption that the electron temperature is equal to the gas temperature. This assumption implies that the ambipolar diffusion coefficient is twice that of the ion, i.e., $D_a = 2D_i$.

[14] From theoretical considerations Bruce H. Mahan [J. Chem.

Phys. **43**, 3080 (1965)] concludes that the temperature dependence of the three-body conversion to form He_2^+ may range between $T^{-5/4}$ at low temperatures to $T^{-1/4}$ at high temperature. G. R. Hays and H. J. Oskam (private communication) have found that the temperature dependence of the reaction-rate constant is small in the range 120–300 °K.

[15] The three-body rate coefficient β for the process $Cs^+ + 2Cs \to Cs_2^+ + Cs$ was estimated by the authors (Ref. 2) to be $\beta \simeq 6\times 10^{-29}$ cm^6/sec. A calculation of the coefficient using the equation derived by Bruce H. Mahan [J. Chem. Phys. **43**, 3080 (1965)] yields a value of $\beta \simeq 10^{-29}$ cm^6/sec. This calculation of β depends upon the charge exchange cross section. A value of the cross section, $Q_{CE} \simeq 7\times 10^{-14}$ cm^2, was extrapolated from the data of W. R. Gentry, Yuan-Tseh Lee, and Bruce H. Mahan [J. Chem. Phys. **49**, 1758 (1968)]. The only other reported value of the coefficient, $\beta \simeq 10^{-26}$ cm^6/sec, was given by N. D. Morgulis and Yu. P. Korchevoi {Zh. Eksp. Teor. Fiz. Pis'ma Red. **9**, 313 (1968) [JETP Lett. **8**, 192 (1968)]}.

[16] J. R. Peterson and D. C. Lorents, Phys. Rev. **182**, 152 (1969).

[17] A. S. Schlachter, D. H. Lloyd, P. J. Bjorkholm, and L. W. Anderson, Phys. Rev. **174**, 201 (1968).

[18] B. L. Donnally and G. Thoeming, Phys. Rev. **159**, 87 (1967).

[19] D. K. Bohme, N. G. Adams, M. Mosesman, D. B. Dunkin, and E. E. Ferguson, J. Chem. Phys. **52**, 5094 (1970).

[20] G. Gioumousis and D. P. Stevenson, J. Chem. Phys. **29**, 294 (1958).

[21] G. E. Chamberlain and J. C. Zorn, Phys. Rev. **129**, 677 (1963).

[22] W. P. Sholette and E. E. Muschlitz, Jr., J. Chem. Phys. **36**, 3368 (1962).

[23] K. L. Bell, A. Dalgarno, and A. E. Kingston, J. Chem. Phys. **36**, 3368 (1962).

[24] P. Langevin, Ann. Chim. Phys. **5**, 245 (1905).

[25] The value of the dielectric coefficient of helium was taken from the *American Institute of Physics Handbook*, 2nd ed. (McGraw-Hill, New York 1963).

[26] A. M. Tyndall, *The Mobility of Positive Ions in Gases* (Cambridge U. P., Cambridge, England, 1938).

[27] A. P. Vitols and H. J. Oskam (private communication).

[28] R. Johnson and M. A. Biondi, Gaseous Electronics Conference, London, Ontario, 1972 (unpublished).

PHYSICAL REVIEW A VOLUME 8, NUMBER 2 AUGUST 1973

Carrier-Frequency Distance Dependence of a Pulse Propagating in a Two-Level System[*]

J. C. Diels[†] and E. L. Hahn
Department of Physics, University of California, Berkeley, California 94720

(Received 11 January 1973)

A study is made of the distance dependence of carrier phase and average frequency of an electromagnetic pulse propagating through a quantum two-level system. Phenomenological differential equations are introduced to describe the distance rate of change of first- and second-moment deviations of the pulse carrier frequency from its original input frequency. In equilibrium the equations predict characteristics of pulse propagation in steady state. For both absorber and amplifier cases, computer plots are presented of the distance dependence of pulse shape, carrier phase, Fourier amplitude, and pulse energy for selected types of homogeneous and inhomogeneous line broadening and for specific input-pulse conditions. Off-resonance formation of a single 2π hyperbolic secant pulse of self-induced transparency may evolve from input-pulse areas less than π, as well as slightly greater than π, accompanied by frequency modulation and pulse breakup. The amplification of pulsed carrier radiation is accompanied by frequency pulling toward resonance. With and without phase modulation, stability conditions for stable pulse propagation are obtained. Either frequency pulling toward or frequency pushing away from resonance is dominant for an absorber, according to the dominance, respectively, of homogeneous or inhomogeneous line broadening. In the slowly-varying-pulse-envelope approximation, a steady-state solution is found for a symmetrically-phase-modulated pulse propagating in an amplifier with scattering losses. The mean carrier frequency for the pulse is displaced off resonance by one linewidth above the resonance transition frequency of a homogeneously broadened system.

I. INTRODUCTION

Little attention has been given to the distance dependence of carrier frequency and phase changes of traveling-wave radiation as it interacts nonlinearly with a medium which contains dipole transitions on or off resonance with respect to the carrier frequency. Cumulative carrier-frequency shifts and spectral changes can result over long distances of propagation. In the far-off-resonance case, significant effects are expected if an infinitely extended medium acts as an amplifier, with excited quantum states populated in excess over lower states by virtue of some external pumping mechanism. The initial off-resonance carrier frequency is expected to pull toward the transition frequency of the inverted system as the distance of propagation increases. In the case of an absorbing medium the spectral changes in the radiation are of quite a different nature, particularly when the radiation is in the form of a pulse. These changes occur if the applied carrier frequency is